

КОНТРОЛЬНЫЙ ЭКЗЕМПЛЯР

45

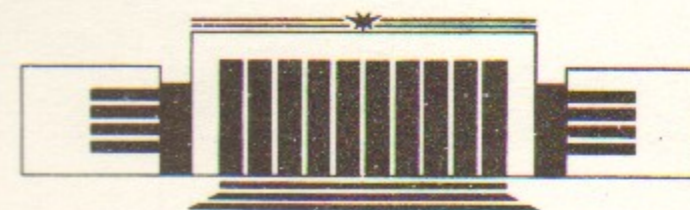


ИНСТИТУТ ЯДЕРНОЙ ФИЗИКИ СО АН СССР

V.M. Aulchenko, B.O. Baibusinov, S.E. Baru,  
A.E. Bondar, A.G. Chilingarov, G.S. Filimonov,  
G. Ya. Kezerashvili, G.M. Kolachev, A.M. Milov,  
T.A. Purlatz, L.V. Romanov, N.I. Root, G.A. Savinov,  
V.V. Serbo, B.A. Shwartz, V.M. Titov, A.E. Undrus,  
A.P. Usov, V.N. Zhilich, A.A. Zholentz,  
H. Calen, S. Kullander

DETECTOR "KEDR" TAGGING SYSTEM FOR  
TWO-PHOTON PHYSICS

PREPRINT 91-49



НОВОСИБИРСК

DETECTOR "KEDR" TAGGING SYSTEM  
FOR TWO-PHOTON PHYSICS

V.M.Aulchenko, B.O.Baibusinov, S.E.Baru, A.E.Bondar,  
A.G.Chilingarov, G.S.Filimonov, G.Ya.Kezerashvili,  
G.M.Kolachev, A.M.Milov, T.A.Purlatz, L.V.Romanov,  
N.I.Root, G.A.Savinov, V.V.Serbo, B.A.Shwartz, V.M.Titov,  
A.E.Undrus, A.P.Usov, V.N.Zhilich, A.A.Zholentz

Institute for Nuclear Physics, Novosibirsk, USSR

H.Calen, S.Kullander

Unit of High Energy Physics of the Uppsala University,  
Sweden

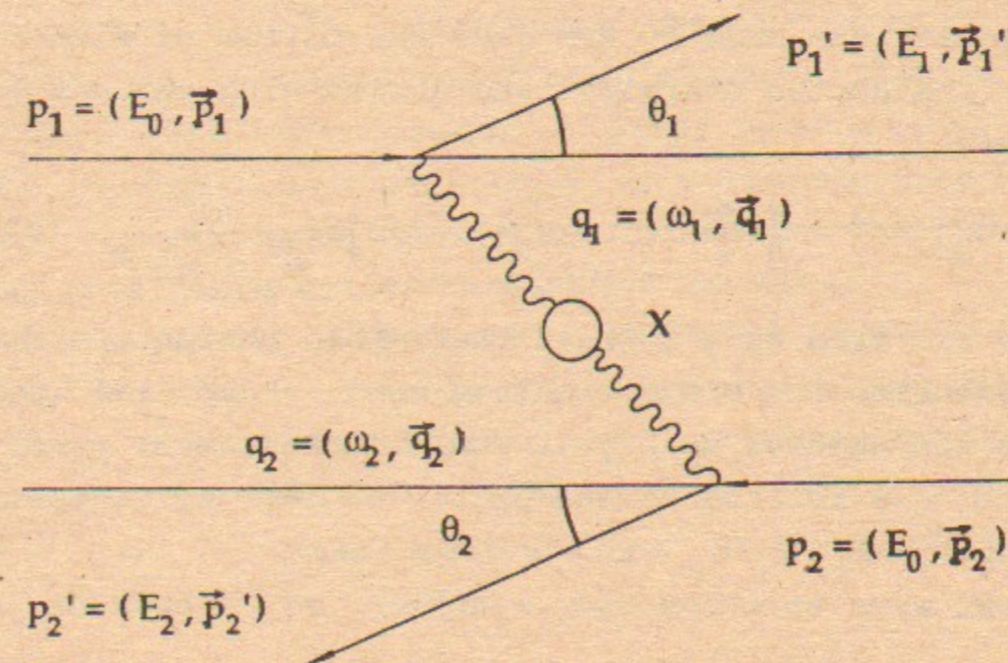
I. INTRODUCTION

Investigation of electron-positron annihilation into final states containing leptons or hadrons plays substantial role in experiments performed at  $e^+e^-$  colliding beams.

However, in addition to the annihilation processes there also exist processes of two-photon production. The cross section of the latter is of higher order in the electromagnetic constant,  $\alpha=1/137$ , than that of the one-photon production. But with the increase of accelerator energy two-photon processes begin to dominate over one-photon ones, because the annihilation production cross section goes down at least as  $1/E^2$  while that of two-photon production rises as  $\ln(E)$ . Besides, the two-photon processes allow to study the objects inaccessible for investigation in the one-photon channel, e.g.  $\gamma\gamma \rightarrow$  hadrons.

The possibility to study  $\gamma\gamma$  interactions at  $e^+e^-$  colliding beams is based on the fact that the field of fast charged particles is rather similar to that of the photon flow. Therefore  $e^+e^-$  beams may be regarded as a source of "photon beams". This statement is the essence of the Equivalent Photon Method (EPM) and may be proved rigorously with Feynman diagram techniques.

The main diagram of  $e^+e^- \rightarrow e^+e^-X$  is shown in the following figure.



The electron and positron radiate virtual photons which produce a C-even state X. Due to the photon propagators of this diagram the cross section is determined by small invariant masses of photons  $q_1^2 = -Q_1^2 = (p_1 - p'_1)^2$ . In other words most of the photons are emitted at small angles and are quasi-real.

The reaction kinematics is determined completely by the initial and final 4-momenta of the scattered electron and positron. At the beam energy  $E_0$  for the description of the  $\gamma\gamma$ -system five parameters are necessary:

$E_1, E_2$  - the energies of the scattered "tagging"-electrons (TE's),

$\theta_1, \theta_2$  - the TE angles with respect to the beam axis;

$\Phi$  - the angle between TE planes.

The kinematic variables of the  $\gamma\gamma$  system may be expressed through TE parameters (omitting the expressions of order  $m_e$ ):

$$\begin{aligned} \omega_{1,2} &= E_0 - E_{1,2}; \\ q_{1,2}^2 &= (p_{1,2} - p'_{1,2})^2 = -2E_0 E_{1,2} (1 - \cos\theta_{1,2}). \end{aligned} \quad (1)$$

The invariant mass of  $\gamma\gamma$  system is

$$W_{\gamma\gamma}^2 = (q_1 + q_2)^2 = 4\omega_1\omega_2 - 2E_1E_2(1 - \cos\theta_1\cos\theta_2 - \sin\theta_1\sin\theta_2\cos\Phi),$$

and for small  $\theta_1$  and  $\theta_2$ ,  $W_{\gamma\gamma}^2$  may be approximated by  $W_{\gamma\gamma}^2 = 4\omega_1\omega_2$ .

The calculations made by EPM give the following distributions for the photon energies and angles with respect to the beam axis:

$$N(\omega) \cdot (d\omega/E_0) \cdot d\theta_\gamma^2 = \frac{\alpha}{\pi} \frac{d\omega}{\omega} (1 - \omega/E_0 + \omega^2/2E_0^2) \cdot \frac{d\theta_\gamma^2}{\theta_\gamma^2 + m_e^2/E_0^2} \quad (2)$$

One can see from this formula that the photon energy spectrum resembles the bremsstrahlung one ( $\sim 1/\omega$ ) and that the photons are emitted mainly at small angles about  $m_e/E_0$ . The TE angles are related to the photon angles by momentum conservation  $\theta_1 = \theta_{\gamma_1} \cdot \omega_1/E_1$  and are also small.

Different ways to study the reaction  $\gamma\gamma \rightarrow$  hadrons at

colliding beams are possible: with detection of both electrons (double-tag), one of them (single-tag) and without tagging (no-tag).

In "no-tag" experiments only the decay products of the hadronic system X are detected. In this case it is necessary, as a rule, to detect all created hadrons in order to get complete information about the  $\gamma\gamma$  kinematics. The hadronic system X, created in the reaction  $e^+e^- \rightarrow e^+e^-X$ , moves longitudinally. Therefore X decay products move mainly at small angles with respect to the beam axis, i.e. in the region where all the detectors have an insensitive area.

The information about the  $\gamma\gamma \rightarrow$  hadrons reaction may be obtained by the detection of tagging electrons. As it is seen from (1), all kinematical variables of the  $\gamma\gamma$  system are expressed in terms of the TE parameters: the photon energy is related to the TE energy by the conservation law  $\omega_1 = E_0 - E_1$ , and the angle  $\theta$  is a measure of  $Q^2$ , i.e. "virtuality". In principle, the detection of both TE's fixes the kinematics of the  $\gamma\gamma$  system, with the precision determined by the resolution of the detection system.

The problems existing in detection of the tagging electrons are connected with their small emission angles. This means that the detection system should be located as close as possible to the beam (especially if one wants to study a low invariant mass region when electrons lose a small fraction of their energy). The important step in the development of detection methods for the study of two-photon processes was made by providing a detector with a special system to tag scattered electrons, electron Tagging System (TS). The review [1] contains a brief description of such systems constructed for a number of different detectors. A tagging system should have high detection efficiency and maximal attainable energy resolution for TE's.

The Institute of Nuclear Physics at Novosibirsk has accumulated some experience in constructing and operating TS's. Here the MD-1 detector, with a transverse magnetic field specially designed for studies of two-photon proces-

ses, was built [2]. The accuracy in TE energy measurement was  $\sigma_E/E \approx 1.5\%$  which allowed to reconstruct invariant masses with  $\sim 100$  MeV precision. The double-tag detection efficiency in the  $\gamma\gamma$  mass region from 1.5 to 3.5 GeV was 10 - 20 %.

This paper describes TS that is now under construction for experiments at the VEPP-4M collider with the detector KEDR[3]. Its parameters are approximately an order of magnitude better than in the previous systems in the measurement accuracy of the  $\gamma\gamma$  system invariant mass. Another advantage of this TS is that in spite of its high detection efficiency it does not inhibit the attainment of maximum luminosity due to its natural inclusion in the interaction region beam optics.

## II . PHYSICS WITH TWO PHOTONS

Let us consider the main problems of the two-photon physics that may be investigated with the help of a TS with good enough detection efficiency and high resolution in invariant mass reconstruction for masses of the  $\gamma\gamma$  system in the 0.5 - 4 GeV region.

### II.1. Study of the total cross section $\gamma\gamma \rightarrow$ hadrons at low $Q^2$ .

The total cross section ( $\gamma\gamma \rightarrow$  hadrons) is a fundamental quantity of soft hadron physics. The study of two-photon creation of hadrons allows to investigate the dynamics of hadrons for a simple initial state.

The difficulty in measurements of the total cross section  $\sigma(\gamma\gamma \rightarrow$  hadrons) in comparison with the one-photon annihilation cross section is due to the fact that the centre of mass energy  $W_{\gamma\gamma}$  is unknown in advance because the photons produce a continuous  $W_{\gamma\gamma}$  spectrum. That means that  $W_{\gamma\gamma}$  should be measured with good precision. Double-tagging allows to do it in a model independent way by reconstruction of the invariant mass with the help of the tagging electron

energies:  $W_{\gamma\gamma}^2 = 4(E_0 - E_1)(E_0 - E_2)$ . The high resolution in the  $\gamma\gamma$  invariant mass is especially important for the low mass region where the resolution of fine structures in the cross section is necessary.

Obviously the pure electrodynamic processes should be suppressed in measurements of the  $\gamma\gamma \rightarrow$  hadrons cross section. For this it is sufficient to detect at least one hadron in the central detector together with the tagging electrons. One of the advantages of the considered TS is the detection of small TE emission angles down to zero degrees. It allows a direct measurement of the cross section for real photons without extrapolation down to  $Q^2=0$ .

### II.2. Study of C-even Resonances with Masses up to 4 GeV

Two-photon physics gives additional opportunities for QCD tests at small distances. Measurement of the  $\gamma\gamma$  width of C-even resonances provides important information about their physical nature and quark structure. A small  $\gamma\gamma$  width is expected for gluonic resonances, e.g. the glueball candidate  $\eta(1440)$  (formerly  $i(1460)$ ). The small two-photon widths for  $a_0(980)$  and  $f_0(975)$  (formerly  $\delta$  и  $S^*$ ) favour the interpretation of these states as novel four-quark resonances or pseudoscalar-pseudoscalar molecules [4,5]. On the other hand the bound states of vector meson pairs would have a large two-photon width [6,7].

The parameters of the TS allow in principle to obtain additional information about the already known resonances (e.g. to measure their width) as well as to look for new possible resonances in a mass region 0.5 - 4 GeV. Again the advantage of the double-tagging method is the direct measurements of the  $\gamma\gamma$  width without knowledge of any specific branching ratios. For example, the  $\gamma\gamma$  width of the above mentioned resonance  $a_0(980)$  is not known, only its product with the  $\eta\pi$  branching ratio has been determined. The direct measurement of  $\Gamma_{\gamma\gamma}$  will allow not only to understand better the nature of this resonance but also to obtain the value of the branching ratio.

Especially interesting are C-even charmonium states. The reason is that the charmed quark represents an intermediate region in QCD and two photon widths of the charmonium states are very sensitive to nonperturbative corrections. Therefore an important task for the TS is the direct measurement of the two-photon width for  $\eta_c(2980)$ ,  $\chi_0(3415)$ ,  $\chi_2(3555)$  from their cross section values. Theoretically the two-photon width of the  $\eta_c$  ( $^1S_0$ -state) can be related to the lepton width  $J/\Psi(^3S_1)$ , because both depend on the quark wave function at the origin  $\Psi(0)$ . Assuming that  $\Psi(0)$  is the same for singlet and triplet states one gets

$$\frac{\Gamma(\eta_c \rightarrow \gamma\gamma)}{\Gamma(J/\Psi \rightarrow l^+l^-)} = \frac{3e_q^4 |\Psi(0)|^2 / m_q^2}{e^2 |\Psi(0)|^2 / m_q^2} = 3e_q^2.$$

Using the measured leptonic width of the  $J/\Psi$ , one obtains  $\Gamma(\eta_c \rightarrow \gamma\gamma) \approx 6.2$  keV. Similar results were obtained using QCD sum rules ( $\approx 4$  keV). On the other hand, the  $\Gamma(J/\Psi \rightarrow \gamma\eta_c)$  is closely related in the framework of QCD with the two photon width of the  $\eta_c$ . The measured rate for the transition  $J/\Psi \rightarrow \gamma\eta_c$  is much smaller than theoretically expected. This is a rather serious problem. The accuracy of the present experimental results for the two-photon width of  $\eta_c$  (PLUTO [8], MARK II [9], MD-1 [10]) is not good enough to clarify this question.

It is also desirable to measure the two-photon width for the P-wave charmonium states  $\chi_0$  and  $\chi_2$ . Crystal Ball results [11], within the errors, do not contradict the two gluon model of hadronic decays and the ratio  $\Gamma_{\chi_0\gamma\gamma} / \Gamma_{\chi_2\gamma\gamma} = 15/4$  expected from spin factors.

For a total collected luminosity of  $100 \text{ pb}^{-1}$  the expected numbers of  $\eta_c$ ,  $\chi_0$ ,  $\chi_2$  events detected by the TS are about 100 events for each resonance providing about 10% accuracy in the measured value of their two photon width.

### II.3. Search for Exotic States

After the observation of the resonance, the first prob-

lem is the definition of its place in the SU(3) classification scheme. The resonances that do not fit in this classification are considered to be exotic states. They may be gluonic states (glueballs), 4-quark states, quark-gluon resonances etc. There exist different models relating a two-photon width to the physical nature of the resonance. The attempts to observe the exotic states in double-tag experiments and to measure its photon width will help to clarify the situation or at least to put up some limits. For example, two-photon production of glueball candidates  $\eta(1440)$ ,  $f_2(1720)$  and  $\xi(2220)$  has not been observed. This qualitatively supports the hypothesis of a small value for the glueball two-photon width at least for  $\eta(1440)$  and  $f_2(1720)$  which are copiously produced in radiative  $J/\Psi$  decays.

The observation of exotic states may allow to recognize 4 quark or mixed quark-gluon resonances.

### III. GENERAL DESCRIPTION OF THE TAGGING SYSTEM

As it was already mentioned in the introduction, the main parameters that characterize the TS and its capabilities are the TE energy resolution (and consequently the resolution in invariant mass of the  $\gamma\gamma$  system) as well as the tagging efficiency in the necessary invariant mass region.

The kinematics of two-photon processes makes necessary the detection of electrons emitted from the interaction point at zero angle to attain high detection efficiency. This can be done by a bending magnet deflecting from the beam those electrons which have lost part of their initial energy. This magnet with the doublet of mini- $\beta$  quadrupoles would be natural to use as a strong focusing magnet-spectrometer for the TE energy measurement. The layout of the TS is shown in figure 1. The TE's coming out from the interaction point pass through the main detector magnet with longitudinal magnetic field, compensating solenoid, quadrupole lenses  $L_1$  and  $L_2$  and bending magnets  $M_1$  and

$M_2$ . The TE is then detected by one of four tagging systems  $TS_1 - TS_4$ , whose basic parameters are presented in the table below. The focusing energy is the energy of TE whose coordinate in the TS, due to the focusing properties of quadrupoles, is independent of the emission angle of the electron at the interaction point.

TS number	Region of tagged energies (fractions of beam energy)	Focusing energy	Dimension of TS (cm)
1	0.39 - 0.59	0.58	7.7
2	0.60 - 0.72	0.66	4.3
3	0.73 - 0.85	0.80	8.9
4	0.85 - 0.98	0.91	15.8

Thus, the mini- $\beta$  quadrupoles at the same time are an essential part of the strong focusing magnetic spectrometer. This solution allows, firstly, to put the lenses closer to the interaction point in order to achieve high luminosity and, secondly, to improve the TE energy resolution as compared to a usual magnetic spectrometer (e.g. the TS of the MD-1 detector).

For particles emitted at a zero angle from the interaction point, the coordinate in the TS is unambiguously determined by their energy. The TE angular distribution, despite its sharp peaking behaviour, destroys this unambiguity. So the nonzero emission angle leads to an error in the energy measurement. But for electrons with focusing energy such an unambiguity is restored. The more the energy differs from the focusing energy, the larger is the error in the energy measurements due to the absence of information about the angle. That is why the TS is divided into four systems, providing a small enough error in the energy measurement over a large TE energy region. The precision of the energy measurement  $\sigma_E/E_0$  vs. TE energy obtained by Monte-Carlo simulation is shown in figure 2. The following factors

are taken into account:

- a) the beam energy spread  $\delta = 8 \cdot 10^{-4}$ ;
- b) the emission angle of TE due to the angular distribution of the two photon production process (simulated in accordance with the EPM formula, see (2) in the introduction);
- c) the angular spread in the beam  $\sigma_{\theta_y} = 5 \cdot 10^{-4}$ ;
- d) the beam size in the interaction point  $\sigma_y = 0.05$  cm;
- e) the coordinate resolution of the TS chambers  $\sigma = 300$   $\mu$ m;
- f) the presence of nonlinear elements (sextupoles of the experimental region for focusing chromaticity compensation).

The double-tag detection efficiency is presented in figure 3. In these calculations the TE was considered as "detected" if it came into the aperture and hit one of the TS's and the reconstructed energy differed from the real one by less than 40 MeV. By this last requirement the events with large emission angles (the long "tails" in the angular distribution) were rejected and only the "useful" efficiency was taken into account.

The resolution in the reconstructed invariant mass of the two-photon system is given in figure 4.

#### IV. COORDINATE SYSTEM AND THE SCINTILLATOR HODOSCOPE

A Monte-Carlo study of the energy resolution, the detection efficiency and the background conditions, allowed to formulate the requirements to the detection part of the system.

- 1) As follows from the analysis of different contributions to the energy resolution (figure 2) the necessary spatial resolution is 0.3 - 0.6 mm.
- 2) It is necessary to measure the entrance angle of the TE into the detecting system with the accuracy of  $\sigma_\theta \approx 2 \cdot 10^{-3}$ . This information is not used directly for the energy reconstruction. By rejecting events with large angles it is possible to suppress considerably the long

tails in the invariant mass distribution (for large initial angles the energy is reconstructed with a large error - more than  $\pm 40$  MeV). Moreover, there are some physical problems not mentioned in part II where it is necessary to know the TE emission angle at the interaction point. That is the study of angular correlation in two-photon production processes. In fact, in this case one needs information not only about the angle in the orbital plane but also about the vertical emission angle. The knowledge of the angle may be used for background suppression. With a spatial resolution of 0.6 mm and a total length of the TS of 30 cm the angular accuracy is  $2 \cdot 10^{-3}$ . Multiple scattering in the entrance window (0.1 radiation lengths) gives approximately the same contribution.

- 3) The detection system has to work with a counting rate of  $2 \cdot 10^6$  Hz.
- 4) Several particles detected simultaneously should be separated.
- 5) The detection system insensitive area at the edge should be small (not more than 5 mm).
- 6) It is necessary to foresee the possibility to "switch off" a region of the TS corresponding to a vertical emission angle at the interaction region of less than some value ( $\approx 0.2$  mrad) for background rejection.

#### IV.1. The Design

Most of these requirements are satisfied in the best way by using a hodoscope of drift tubes (DT's). Each TS includes one hodoscope designed as an independent module which contains six detecting planes (figure 5). The plane is made of two rows of stainless steel drift tubes with 6 mm diameter and 90  $\mu$ m wall thickness. The pitch of the tubes in one row is 8 mm, rows are shifted one relative to another by 4 mm. Anode wires are stretched with 0.3 mm shift relative to the tube centre and the sign of the shift is different in adjacent layers. This avoids left-right ambiguities in the

track reconstruction. In the  $TS_1$ ,  $TS_2$  and  $TS_3$  modules each row contains 12 DT's. The  $TS_4$  module has a 24 tube row. The total number of tubes in the TS is 1440.

#### IV.2. Electronics

Each DT is read out by a preamplifier and a shaper located on the hodoscope. The rise time of the output signal is 5-7 nsec, the decay time is about 25 nsec. The front-end electronics is arranged into independent blocks of 12 channels, which are mounted directly on wire pins. Logical signals from the front-end blocks are fed to an intermediate electronics block for matching to the digitizing electronics. The analog to digital conversion is made by electronics modules made in a special standard [12]. Time intervals are measured by a direct counting method. The time discreteness is 2 nsec. The threshold of the electronics is  $7 \cdot 10^{-15}$  Q.

The average spatial resolution in the DT's measured with a prototype of 11 tubes was found to be about 300  $\mu$ m at a gas gain of  $5 \cdot 10^5$ . By increasing the gas gain up to  $2 - 4 \cdot 10^6$ , a resolution of  $\sigma \approx 200$   $\mu$ m is easy to obtain.

#### IV.3. Radiation Hardness and Gas System

The most crucial problem which should be solved in the TS design is the ability of the system to work for the long times in high counting rate conditions. For example, the rate of SBS (Single BremsStrahlung) electrons in a layer of 5 mm thickness around the beam orbit plane reaches 200 kHz. To manage this problem the system will be operated at the lowest possible gas gain. The possibility of hodoscope movement is provided for, which allows to decrease the density of irradiation approximately by 10 times.

To study the problem of radiation hardness several single-tube modules were made of the materials that will be used in the TS modules. The test tubes were irradiated using a  $^{90}\text{Sr}$  source and an X-ray tube.

During irradiation of a DT which is flowed by an  $\text{Ar-CO}_2$

mixture a drop of the signal amplitude with a rate of  $300\% \cdot \text{cm}/Q$  is being observed which makes this mixture unsuitable for the system. At present a  $90\% \text{CF}_4 + 10\% \text{C}_4\text{H}_{10}$  gas mixture looks quite satisfactory. In this case a dose of  $5 Q/\text{cm}$  does not result in any noticeable gain variation.

The reproducibility of the irradiation effects and the influence of the irradiation rate have not yet been sufficiently studied.

#### IV.4. Scintillator Hodoscope

For rejection of a narrow region in the vertical direction near the horizontal plane, each TS is equipped with a hodoscope of scintillator bars. A hodoscope element is a counter provided with a PM tube of type FEU-60. Each hodoscope consists of 10 counters, 5 above and 5 below the horizontal plane. The regulated gap between the upper and the lower counters determines the region to be rejected.

Moreover, the time for the passage of the particle through the counter is measured. This information may be used for the beam background rejection.

#### V. BEAM ORBIT STABILIZATION

A pick-up system of the VEPP-4 collider monitors the beam position with a relative accuracy of about  $0.1 \text{ mm}$  but only when one of the beams is present. For the orbit stabilization in the interaction region with the colliding beams the synchrotron radiation (SR) from the bending magnets is used.

The narrow SR beam obtained with the help of  $1 \text{ mm}$  collimator passes between the electrodes of two plane ionization chambers. They measure its shifts in vertical and orbit planes. The signal electrode of the chamber is divided into two parts. The separation line is going by  $45$  degrees relative to SR beam direction. The change in the orbit position leads to a shift of the SR beam that influences the ratio of signals from the chamber electrodes. It is measured by the integrating voltmeter with a relative precision

$10^{-4}$ . Keeping this ratio constant will allow to stabilize the orbit position with  $50 \text{ micron}$  accuracy (in the radiation point). It is planned to control the beam position by this method in 4 points. The distances between the radiation point and collimator as well as between the latter and the ionization chambers are  $4 - 7 \text{ m}$ .

Ionization chambers are placed in the volume filled with xenon at  $1 \text{ atm}$ . Their operation is monitored by measurement of the current from additional rectangular electrodes. The signal electrodes are surrounded by guard rings. The SR intensity is adjusted by the thickness of a cooled absorber placed immediately after the collimator so that the current in the chambers is about  $1 \text{ microampere}$ .

#### VI. LASER-OPTICAL SYSTEM FOR TS CALIBRATION

The absolute calibration of the energy measured by the tagging system becomes very important because of the high relative accuracy of the tagging electron energy at the level  $2 \cdot 10^{-3}$ . The ideal opportunity for this could be to obtain electrons with the energy lying in the range  $(0.4 - 0.98) \cdot E_0$  and known with  $0.1\%$  accuracy. The real way to have this opportunity is to use the process of the backward Compton scattering where electrons lose a part of their momenta giving it to the electromagnetic wave. The energy spectrum of the electrons after interaction has a sharp edge depending on the laser and charged particle beam parameters. The method of the backward Compton scattering of laser photons at the electron beam in storage rings was actively developed at Novosibirsk INP during the last years [13, 14]. Because of high coherence of the light source a limitation on the absolute calibration accuracy is connected mainly with the electron beam parameters: its energy and angular spread in the region of its interaction with laser photons. This method allows the absolute calibration of the TS with an accuracy not worse than  $10^{-3}$  in the wide enough range of the particle momenta by using several harmonics of laser



radiation. Laser-Optical System of Calibration (LOSC) will allow to obtain necessary losses of electron momenta in the middle of the experimental region. Moreover, the use of this method will give the opportunity of fast calibration without the change of the collider working mode.

#### VI.1 Choice of the Main Parameters

The choice of the set-up parameters is determined by the existence of four detection systems  $TS_1 - TS_4$  (figure 1) and the desire to calibrate each of them independently. The range of the particle momenta detected by each system is presented in the table in Part III. The wide range of the laser light wave length from infrared up to UV is necessary to obtain in Compton interaction the scattered electrons and positrons with sharp low momenta edges in each detection system region.

The curves for the relative electron momenta after the electron-photon interaction vs. their initial energy are shown in figure 6 for different harmonics of the laser light. It can be seen that after the interaction with the first laser radiation harmonic having the energy 1.17 eV the electrons keep more than 90% of their initial momentum. Therefore the lower edge of electron spectra will lie in the detection region of  $TS_4$ . The second harmonic photons will allow to calibrate  $TS_4$  and  $TS_3$  depending on the collider beam energy.  $TS_3$  and  $TS_2$  may be calibrated by the third and the fourth harmonics of laser radiation. The calibration of the closest to the interaction region  $TS_1$  by the edge of the spectra is confronted with considerable difficulties connected with the obtaining of high radiation harmonics and their absorption in the quartz glass of the set-up optical elements. But due to the fact that  $TS_1$  and  $TS_2$  are situated after the same magnet  $M_1$  (see figure 1) the calibration of  $TS_2$  only is enough.

There are also limits for the length of a laser photon bunch. The duration of the light pulse should not exceed 30 ns for zero angle of electron-photon collisions because the

region of light and particle interaction should be situated between the lenses. To fulfil this requirement the system is equipped by the acoustic-optical Q-factor modulator placed inside the laser resonator (see figure 7) and synchronized with a revolution frequency in the collider. Moreover, the opportunity of the collision of laser radiation with the particle beam at the angle 15 mrad is foreseen in the set-up that will allow to emit the scattered electrons from the necessary place of the collider interaction region with the length of electron-photon interaction area about 10 cm. This gives the opportunity to calibrate the TS by the electrons emitted directly from the VEPP-4M interaction region.

The optical system should form the photon beam with 1 mm diameter and provide means of its precision positioning in the region of interaction with the electron beam. It will allow to obtain 0.01 - 0.1 gamma quantum per one interaction act depending on the laser harmonic used. For such operation mode the probability of the simultaneous emission of two photons is low. Moreover, the work with 1 kHz repetition rate and laser photon bunch synchronization allows to decrease by almost 1000 times the background from the residual gas bremsstrahlung.

#### VI.2 Description of the Optical System

Three solid state pulse lasers generating photons with 1 kHz repetition rate, 70 ns pulse duration and 1.17 eV photon energy are supposed to be used as the sources of light radiation (figure 7). Special devices form the harmonics of the main laser line with the energies 2.34, 3.51, 4.68 eV. The choice of the work mode is performed by the rotating mirror MM. The possibility to control and measure the polarization (Pockels cell and polarimeter) is foreseen for experiments with the polarized electron and positron beams at VEPP-4M. A photomultiplier PMT serves for synchronization of the detecting apparatus by the laser light pulse.

The system of lenses and mirrors sends the laser radiation into the vacuum chamber and forms a necessary

size of the light spot in the place of the electron-photon interaction (figure 1). The calibration from the positron direction is done when the mirror C3 is removed. To organize the collision of photons with electrons or positrons at 15 mrad angle the mirrors C4, C7 can also be removed inside the vacuum chamber.

High energy gamma-quanta leave the vacuum chamber through the berillium windows and are detected by apparatus measuring their energy and coordinate distribution.

### VI.3 Optical System Capabilities

As was mentioned in point VI.1, the LOSC should provide the intensity of the emission of scattered electrons at the level 0.01 - 0.1 particle per interaction act. Moreover this emission should go out of the region between the lenses. The fulfilment of this requirement depends crucially on the possibility to create a short laser pulse with high density and to place it precisely in the interaction point of the collider so that the centres of the electron and photon beams coincide. The case when these requirements are met may be considered as the ideal one. The calculations show how the total intensity of emission of scattered electrons depends on the duration of the laser pulse in the "ideal" case (curve 1 at figure 8). The above mentioned conditions may be fulfilled only with some precision which is allowed by the optical system. It is supposed that we shall be able to control the beam position in the interaction point with an accuracy 30 microns and to put the light bunch in the interaction area with a precision  $\pm 0.5$  m. With this we have to obtain more than 90% of maximum attainable intensity of the electron emission for given duration of the laser pulse (curve 2 at figure 8). The curve 3 shows which part of the electrons will be emitted from the region between the lenses. As can be seen from the figure, more than 50% of the electrons are emitted from the region of interest. The curve saturates when the length of the laser pulse becomes larger than the collider straight section length. But for precise

TS calibration electrons should lose their energy before coming into the magnetic field of the lenses and for this purpose the option of collision at 15 mrad angle is foreseen.

## VII. BACKGROUND CONDITIONS

### VII.1. Synchrotron Radiation Background

The spectrometer bending magnets with large magnetic fields produce synchrotron radiation (SR). The SR photons hit the central detector and the tagging system chambers. To diminish the SR background down to an acceptable level special measures are taken: the edge part of the bending magnet has a field several times lower than in the main part of the magnet. A special system of SR absorbers and scrapers is developed so that the photon has to scatter at least twice to come into the detector. The thickness of the foil protecting the tagging system detectors from SR is 0.1 radiation length. Estimates taking into account photon reflection from SR absorbers, the thickness of the Pb input window and the probability of photon interactions with the gas predict a background rate for  $TS_1$  (where SR background is maximal) of 0.02 photons/turn/10mA.

### VII.2. Background from Single Bremsstrahlung and Coulomb scattering on Residual Gas

Beam electrons which lose energy because of these processes in the straight section before the tagging system bending magnets are swept by the magnetic field and hit partly the  $TS_1$  and the  $TS_2$  detectors. For a pressure,  $P$ , of  $2 \cdot 10^{-9}$  torr and a beam current,  $I$ , of 10 mA the background rate in the systems closest to the interaction point will be about 5 kHz.

### VII.3. Single Bremsstrahlung at Colliding Beam

The main source of background in the tagging system is single bremsstrahlung (SBS) at colliding beam. For detection

of tagged electrons with an emission angle down to zero this problem becomes very serious.

The cross section of this process (for one side from the interaction point) is

$$\frac{d\sigma}{d\omega} = \frac{16}{3} \alpha \cdot r_0^2 \ln \gamma \cdot \frac{1}{\omega} = 6.0 \cdot 10^{-26} \cdot \frac{1}{\omega} \text{ cm}^2.$$

To be detected in the tagging system the electron has to lose an energy from  $\omega_{\min} = 0.02E_0$  up to  $\omega_{\max} = 0.60E_0$ , where  $E_0$  is the beam energy. Then the total detection cross section for electrons from SBS at one side of the tagging system is

$$\sigma = 2.0 \cdot 10^{-25} \text{ cm}^2.$$

For the luminosity  $L = 10^{31} \text{ cm}^{-2} \text{ s}^{-1}$  the background TE counting rate is  $dN/dt = 2.0 \cdot 10^6 \text{ Hz}$  that is about 2 electrons/collision for a beam revolution frequency of 1 MHz. So for  $2 \times 2$  bunches in the collider and  $2 \cdot 10^{31} \text{ cm}^{-2} \text{ s}^{-1}$  luminosity the tagging system will detect in average  $\bar{n} = 2.0$  electrons from SBS at each side.

Let us suppose that information from the central detector allows to select two-photon hadron production events. But for each such event in addition to tagging electrons the electrons from SBS will be detected with high probability. If we have no way to define which electrons originated from the two-photon process we have to consider all possible electron-positron pairs. The combinatorial background will be very large in this case.

The average double-tag efficiency is  $\hat{\epsilon} = 0.22$ . The one side detection efficiency may be estimated roughly as  $\sqrt{\hat{\epsilon}}$ . The effect/background ratio may be understood with the help of the following simple model.

For each  $\gamma\gamma$  event at every side from interaction point there will be  $\sqrt{\hat{\epsilon}}$  TE's and  $\bar{n}$  background electrons detected. The number of combinations of TE's for the invariant mass reconstruction is

$$\left( \bar{n} + \sqrt{\hat{\epsilon}} \right)^2 = \underset{\text{effect}}{\hat{\epsilon}} + \underset{\text{background}}{\bar{n}^2 + 2\bar{n}\sqrt{\hat{\epsilon}}}.$$

Therefore the background to effect ratio is

$$\frac{\text{Background}}{\text{effect}} = \frac{\bar{n}^2 + 2\bar{n}\sqrt{\hat{\epsilon}}}{\hat{\epsilon}} \approx 30.$$

for  $\bar{n} = 2.0$ . So for a typical luminosity  $L = 2 \cdot 10^{31} \text{ cm}^{-2} \text{ s}^{-1}$  the SBS gives a combinatorial background exceeding 30 times the number of useful events and this ratio increases as  $L^2$ .

One of the main tasks for the tagging system will be the search and measurement of the two photon width of narrow C-even resonances in the mass region 1 - 4 GeV. The cross section of the reaction  $\gamma\gamma \rightarrow \text{hadrons}$  represents a nonresonant smooth curve with narrow peaks on it. Having in mind that the resonances are small in comparison with nonresonant cross section beneath them the following rather specific parameter was chosen to compare different methods of background suppression. It is "time needed to collect the necessary statistics for the detection of a hypothetical resonance at a given confidence level". Let us consider how to define this time.

Let  $\sigma_{\text{res}}$  be the cross section of resonance creation at mass  $\mu_{\text{res}}$ , and let  $\lambda\sigma_{\text{res}}$  be the nonresonant hadron production cross section for hadron invariant mass  $\mu_{\text{res}}$  ( $\lambda \gg 1$ ). Then without SBS background the number of detected resonant events will be  $N_R = \sigma_{\text{res}} L t \epsilon$ , and the nonresonant ones:  $N_{NR} = \lambda\sigma_{\text{res}} L t \epsilon$ , where  $\epsilon$  is the detection efficiency for  $W_{\gamma\gamma} = \mu_{\text{res}}$ . Let us define  $p_0 = N_R / \sqrt{N_{NR}} = \sqrt{\sigma_{\text{res}} L t \epsilon / \lambda}$  to be the ratio of the number of resonant events to the statistical fluctuation  $\sqrt{N_{NR}}$  of the nonresonant one. In the case of the real background a similar parameter  $p$  may be defined as the ratio of the resonant event number left after background rejection  $N'_R$  to the fluctuation of the nonresonant event number  $\sqrt{N_{bR}}$  with accidental coincidence background taken into account. The ratio  $(p_0/p)^2$  shows how much the statistics should be increased to obtain with background the same confidence level as without it.

Let us define  $L_0$ , as a luminosity at which  $\bar{n} = 1$ . In our case  $L_0 = 1 \cdot 10^{31} \text{ cm}^{-2} \text{ s}^{-1}$ . We are interested in the time which is necessary to collect enough information to reach a

given confidence level. Without any background  $t = \frac{p^2 \cdot \lambda}{\sigma_{res} \cdot cL} = t_0 \cdot \frac{L}{L_0}$ , where  $t_0 = \frac{p^2 \cdot \lambda}{\sigma_{res} \cdot cL_0}$  is the time necessary to reach the confidence level  $p$  at the luminosity  $L_0$ . This ideal dependence of  $t$  (in units of  $t_0$ ) vs.  $L$  in absence of SBS background is shown in figure 9 by the dashed line. The necessary time is obviously decreasing with an increase of luminosity.

When there is a background from the accidental coincidence with SBS events  $t/t_0 = \frac{1}{(L/L_0)(p/p_0)^2}$ . The ratio  $(p/p_0)^2$  is in general case a complicated function of the luminosity and may be found by Monte-Carlo simulation. Assuming that the spectra of the background and nonresonant two-photon production are similar (due to their similar photon energy spectra of the bremsstrahlung type  $\sim 1/\omega$ ), one can obtain the simple expression for  $t/t_0$  without any background suppression ( $N_R' = N_R$ ). Repeating the above made calculations one can get

$$(p/p_0)^2 = N_{BR}/N_{NR} = \frac{\text{effect} + \text{background}}{\text{effect}} = \frac{(\bar{n} + \sqrt{\hat{\epsilon}})^2}{\hat{\epsilon}}$$

from which, using  $\bar{n} = L/L_0$ , one obtains

$$t/t_0 = (L_0/L) \cdot \left( \frac{\bar{n}}{\sqrt{\hat{\epsilon}}} + 1 \right)^2 = (L_0/L) \cdot \left( \frac{L}{L_0 \sqrt{\hat{\epsilon}}} + 1 \right)^2.$$

So with SBS background the  $t$  vs.  $L$  dependence is quite different (this curve is also shown in figure 9). It has a minimum at  $L_{opt} = 0.5 \cdot 10^{31} \text{ cm}^{-2} \text{ s}^{-1}$ . For  $L > L_{opt}$  the necessary time is increasing with luminosity because of the sharp increase of the combinatorial background. The luminosity planned for VEPP-4 is  $(2 - 4) \cdot 10^{31} \text{ cm}^{-2} \text{ s}^{-1}$ . From the curve in the figure 9 it is clear that without SBS background suppression there is no sense in having such a luminosity for this particular tasks: the time of data collection would only be increased.

Let us discuss the different methods of SBS background suppression and compare them using the  $t/t_0$  parameter.

### VII.3.1. Rejection of the Horizontal Region

The TE emission angle is related to the angle of the corresponding  $\gamma$ -quantum by the momentum conservation. The angular distribution of SBS photons:  $d\theta_\gamma^2 / (\theta_\gamma^2 + 1/\gamma^2)^2$  is even more sharp compared with that of photons from  $\gamma\gamma$  processes:  $d\theta_\gamma^2 / (\theta_\gamma^2 + 1/\gamma^2)$ . This fact can be used for background suppression. One can improve the effect/background ratio by rejecting the events with the vertical angle  $|\theta_{x0}| < \theta_0$ , but with a decrease in TE detection efficiency. The choice of  $\theta_0$  is determined by the angular spread at the interaction region. For each value of luminosity there exists a  $\theta_0$ , which is optimal from the point of minimal data collection time. The  $t$  vs.  $L$  dependence for this method of background suppression is also shown in figure 9. The main disadvantage of this method is a significant loss in detection efficiency.

### VII.3.2. Determination of the Interaction Point from the Time-of-flight of the Tagging Electrons

A possible method of SBS background suppression is the measurement of time-of-flight for TE's. The method uses the fact that the bunch has a non zero length ( $\sigma_1 \approx 5 \text{ cm}$ ) and TE's should originate from the same point as hadrons in the central detector. The vertex position should be determined by the measurements in the central detector. Then the background may be suppressed by measurement of the TE emission point position by their TOF and by comparison of this position with that of the event vertex. If at least one of these TE's belongs to the background the emission point does not coincide with the vertex found by the central detector. Obviously the quality of the suppression by this method is determined by the time resolution of the TOF counters installed behind the detection system. Work on these counters is in progress now. The resolution obtained with a prototype is 30 picoseconds. In figure 9 the  $t$  vs  $L$  dependence for this TOF resolution is shown.

### VII.3.3. Determination of Energy Deposition and Momentum Direction in the Central Detector

Some part of the background may be suppressed with the help of information about the decay products detected in the central detector. For quantitative estimates a detailed simulation is necessary. It has not been done yet. Nevertheless one can say that this method cannot allow radical background suppression because due to the specific kinematics of  $\gamma\gamma$  processes, as a rule, not all the decay products of the two-photon system are detected.

### VII.3.4. Detection of SBS Photons

The most proper way to suppress background would be to detect SBS photons and measure their energy. In the SBS process the sum of electron and photon energies is equal to the beam energy. Then one can reject the TE's for which photons with corresponding energies are detected.

But the measurement of SBS photon energies separately for each photon is difficult: in each  $e^+e^-$  collision several photons are emitted from the interaction region in each direction in accordance with the SBS cross section given above, and all of them come out at very small angles to the beam axis. Therefore the usual calorimetric measurement gives only a sum of the SBS photon energies including the photons for which the electrons fall outside the tagging system acceptance. One can use this information in order to suppress background by selecting among the detected electrons such a set for which the sum of missing energies is equal to the energy deposited in the calorimeter.

#### VII.3.4.1. Zero Angle Calorimeter: Scintillator Sandwiches

For SBS background suppression, scintillator sandwiches will be installed at both sides of the interaction region for detection of photons emitted from the interaction region at small angles. The general layout of this sandwich is shown in figure 10. It consists of 4 modules having 25 layers each (1 mm Pb and 5 mm of plastic scintillator per

layer). Therefore the total calorimeter thickness is  $18 X_0$  ( $X_0$  = radiation length). The light collection is done with the help of plane-parallel plexiglass light guides coupled to PM FEU-110 (4 PM's per module).

In figure 9, the  $t/t_0$  vs.  $L$  dependence is shown for a case where background suppression is based on calorimeter measurements only. The calorimeter energy resolution in this simulation was supposed to be  $\sigma_E/E = 8.0\%/ \sqrt{E}$ .

One can see that this gives considerable improvement in comparison with the situation without background suppression. The optimal luminosity is about  $1 \cdot 10^{31} \text{ cm}^{-2} \text{ s}^{-1}$  and the optimal time is 5 times lower.

#### VII.3.4.2. Pair Spectrometer with Silicon Strip Detectors

For more effective background suppression it is necessary to measure each photon energy separately. It can be done with the help of a pair spectrometer consisting of many thin converters in a magnetic field and with a coordinate detector system. Photons will be converted in such a spectrometer to  $e^+e^-$  pairs (different photons typically in different converters). The photon energy is determined by the curvature of electron and positron tracks in the magnetic field.

The converter thickness is determined by the following conditions. On one hand the total spectrometer length is limited ( $\approx 3$  m), and for at least 90% conversion efficiency the total thickness should be  $3X_0$ . On the other hand the converter must not be too thick, otherwise the produced  $e^+$ ,  $e^-$  will lose their energy in the converter by bremsstrahlung which will deteriorate the energy resolution. The compromise between these contradicting conditions leads to the conclusion that the optimal converter thickness is  $\approx 0.10X_0$ . Therefore the spectrometer should contain 30-40 converters with about 10 cm separation distance. The transverse dimensions of the converters are determined by the beam angular spread and the distance between the spectrometer and interaction region ( $\approx 20$  m). The minimal transverse dimension

of the converter is  $\pm 1.5$  cm. At 10 cm distance between the converters the electron with 1 GeV energy does not turn enough in 2.0 T magnetic field to pass the next converter and will hit it losing the energy and producing new particles in the spectrometer. Therefore the curvature should be measured at the position between two adjacent converters. The limited length for curvature measurement requires high coordinate resolution detectors. Silicon strip detectors with  $50 \times 50$  mm sensitive area and  $50 \mu\text{m}$  pitch look suitable for this task. Then the pair spectrometer becomes rather compact (see figure 11): the detectors are placed after each converter and in the middle between two converters. Thus three points for curvature measurement between two converters are obtained. Behind the spectrometer at 2 m distance there is a calorimeter (scintillator sandwich) detecting the nonconverted photons.

The energy resolution for conversion  $e^\pm$  is determined by their multiple scattering in the Si detector plates and the precision of the coordinate measurements. In addition some error in photon energy measurement appears due to radiation losses in  $e^\pm$  energies in the converter media.

Monte Carlo simulation was performed to study the energy resolution of the pair spectrometer and to make the optimal choice of converter thickness (there is some advantage in making converters with different thickness growing with the coordinate from the interaction region). With the help of the GEANT program [15] simulating the passage of particles through the matter, the curve showing the quality of SBS background suppression by the pair spectrometer was obtained (figure 9). The reconstruction process inaccuracies (wrong track recognition etc.) are also included. The energy resolution of the pair spectrometer for a single photon is shown in figure 12.

So the use of a pair spectrometer for SBS photon detection would be quite adequate for background suppression in two-photon events for the planned parameters of VEPP-4M. By using simultaneously the TOF information for the tagging

electrons it is possible to come closer to the ideal curve corresponding to the absence of background (dashed curve in figure 9).

#### VIII. CONCLUSION

A tagging system for studies of two-photon physics is described. It is a part of the multipurpose detector KEDR and  $e^+e^-$  collider VEPP-4M at Novosibirsk. Use of some accelerator magnetic structure elements allows to obtain high double tagging efficiency and resolution in  $e^+$  and  $e^-$  energies. Double tag method giving the two-photon mass without reconstruction by its decay products has serious advantages and is complementary to the commonly used "no-tag" and "single-tag" approaches. It is expected to be especially useful for measurements of the two-photon width of resonances and the total cross-section of two gammas into hadrons.

The main background comes out of single bremsstrahlung. Several methods of its rejection are discussed in the paper.

#### IX. ACKNOWLEDGEMENTS

The authors would like to express their sincere gratitude to S.I. Eidelman and K. Fransson for the fruitful discussions and the generous help in the manuscript preparation.

## REFERENCES

1. H. Kolanoski. Two-Photon Physics at  $e^+e^-$  Storage Rings. Springer Tracts in Modern Physics 105. Berlin-Heidelberg-New-York-Tokyo 1984.
2. A.E. Bondar et al. Preprint INP 82-17, Novosibirsk 1982.
3. V.V. Anashin et al. Proceed. of the Int. Symp. on Coordinate detectors, Dubna, 1987 p.....
4. N.N. Achasov, S.A. Devyanin and G.N. Shestakov. Phys.Lett. 108B (1982) 134, Z.Phys. C16 (1982) 55.
5. J. Weinshtein and M. Isgur, Phys.Rev. D27 (1983) 588.
6. N.N. Achasov, S.A. Devyanin and G.N. Shestakov. Z.Phys. C27 (1985) 99.
7. B.A. Li and K.F. Liu, Phys.Rev Lett. 57 (1986) 3245.
8. PLUTO Coll., Ch. Berger et al., Phys. Lett. 167B (1986) 120.
9. S. Cooper, Proceedings of the XXIII Intern. Conf. on High Energy Physics, Berkeley, 1986.
10. A.E. Blinov et al., Novosibirsk preprint 86-107, 1986.
11. R.A. Lee, Thesis Stanford University SLAC-282 UC-34D, 1985.
12. V.M. Aulchenko, S.E. Baru, G.A. Savinov. Preprint INP 88-29, Novosibirsk 1982.
13. A.A. Kazakov, G.Ya. Kezerashvili, L.E. Lazareva et al. Proceed. of IX All-Union Workshop on High Energy Particle Accelerators, v. II, p.268, Dubna, 1985. The Second International Seminar on Spin Effects in High Energy Physics, p.140 Serpuchov, 1985
14. S.A. Belomestnykh et al. Proc. of XI All-Union Workshop on High Energy Particle Accelerators, v.II, p.410, Dubna, 1989.
15. R. Brun et al., GEANT3, DD/EE/84-1, 1987.

## FIGURE CAPTIONS

Fig.1 Interaction region of VEPP-4M collider. S - solenoid, L - quadrupole lenses, M - bending magnets, TS - tagging systems for electron detection, C - optical mirrors, F - optical lenses.

Fig.2 Energy resolution for tagging electron. The contribution of TS coordinate resolution ( $\sigma=300 \mu\text{m}$ ) only is shown by the dashed line.

Fig.3 Double tag efficiency vs.  $\gamma\gamma$  invariant mass.

Fig.4 Two-photon invariant mass resolution.

Fig.5 Coordinate system and scintillator hodoscope.

Fig.6 The relative momentum of scattered electrons vs. their initial energy for compton interaction with different harmonic laser photons. The first harmonic energy is 1.17 eV.

Fig.7 The LOSC optical system elements. AOM - Acoustic-optical Q-factor modulator, D, T, Q - the transformers to the second, third and fourth harmonics respectively. For details - see text.

Fig.8 Relative intensity of scattered electrons vs. laser pulse duration. The curve 1 - ideal case intensity. The curve 2 shows what part of ideal intensity can be achieved in real case. The curve 3 - the part of scattered electrons emitted from the region between the lenses.

Fig.9 Time (in relative units) of necessary statistics collection vs. luminosity.

The curves:

1 - without SBS background suppression;

- 2 - with a cut around the horizontal plane;
  - 3 - TOF measurement with  $\sigma = 30$  ps;
  - 4 - with scintillator sandwich;
  - 5 - with pair spectrometer;
- the dashed line - ideal case in absence of any background.

Fig.10 Scintillator sandwich.

Fig.11 Lay-out of pair spectrometer with semiconductor detectors.

Fig.12 Energy resolution for a photon producing a pair in the spectrometer.

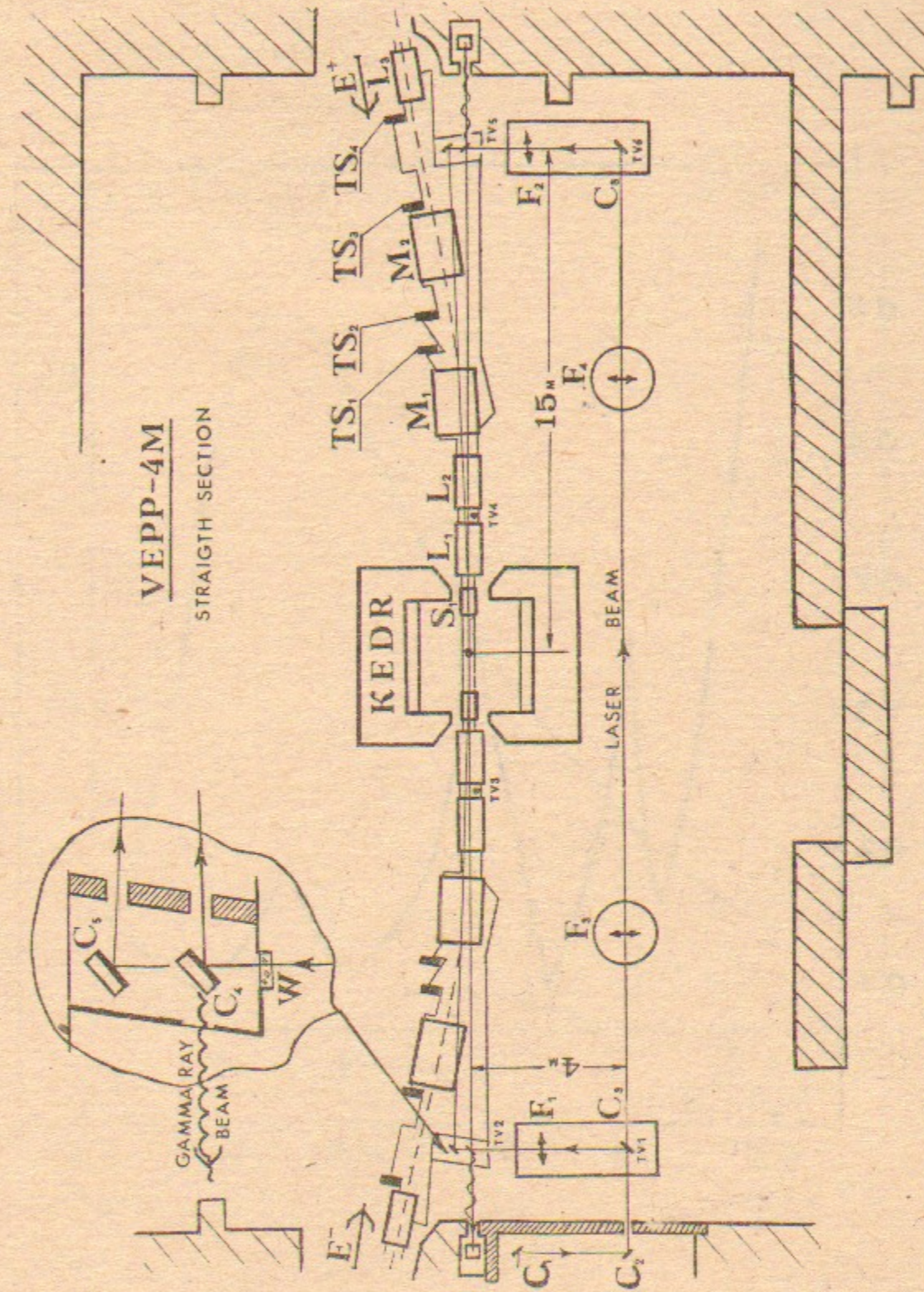


Fig. 1



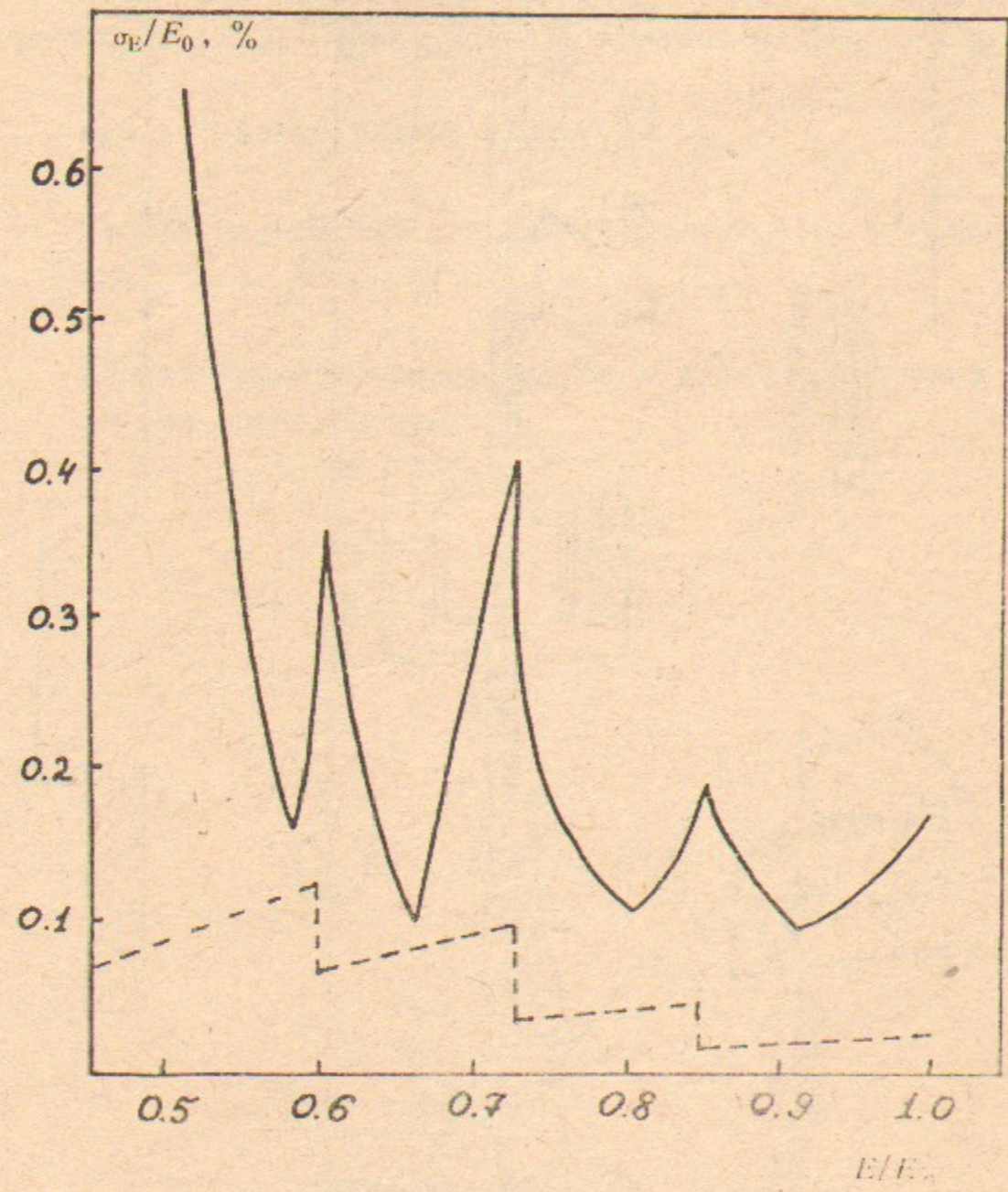


Fig. 2  
32

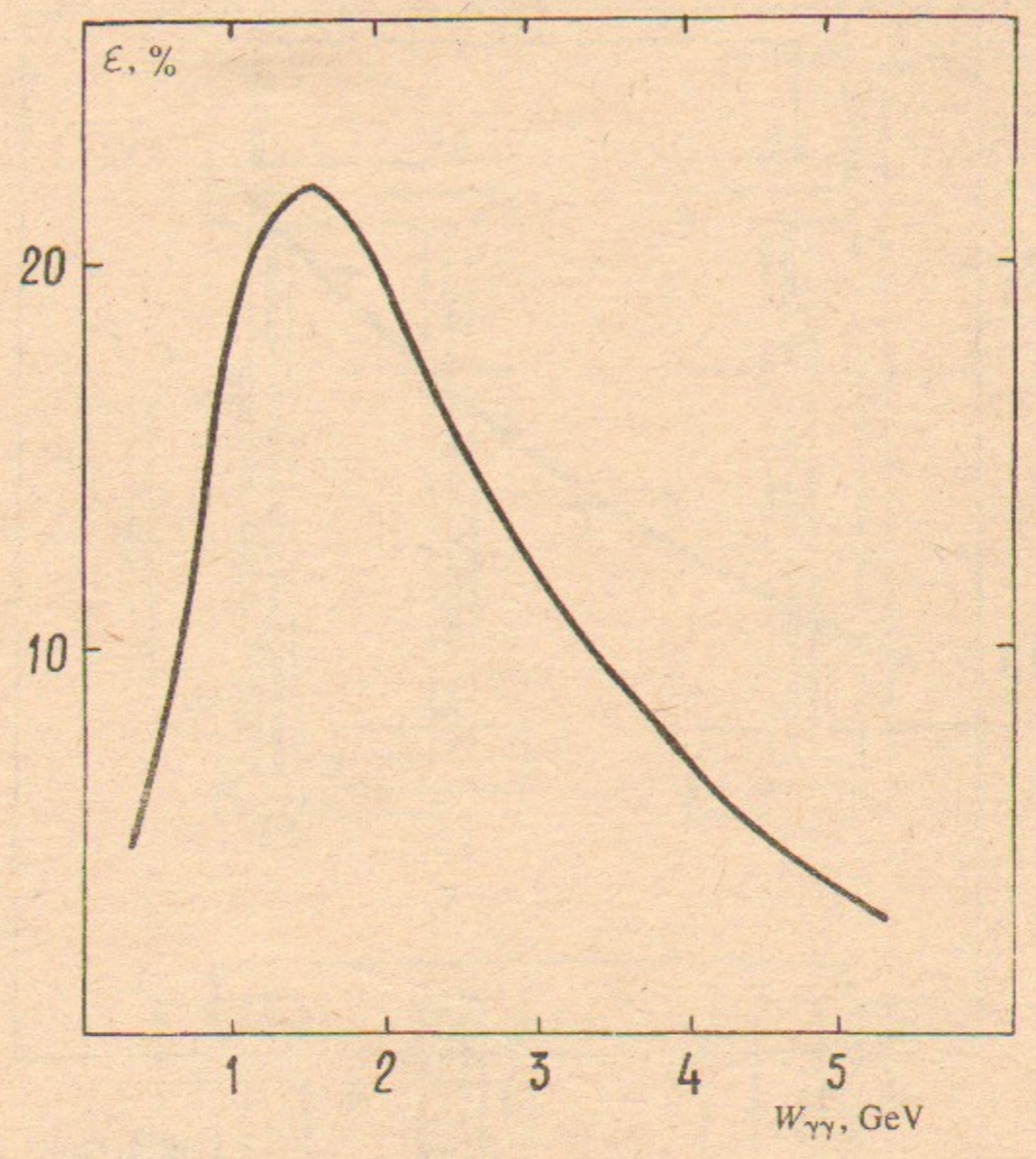


Fig. 3  
33

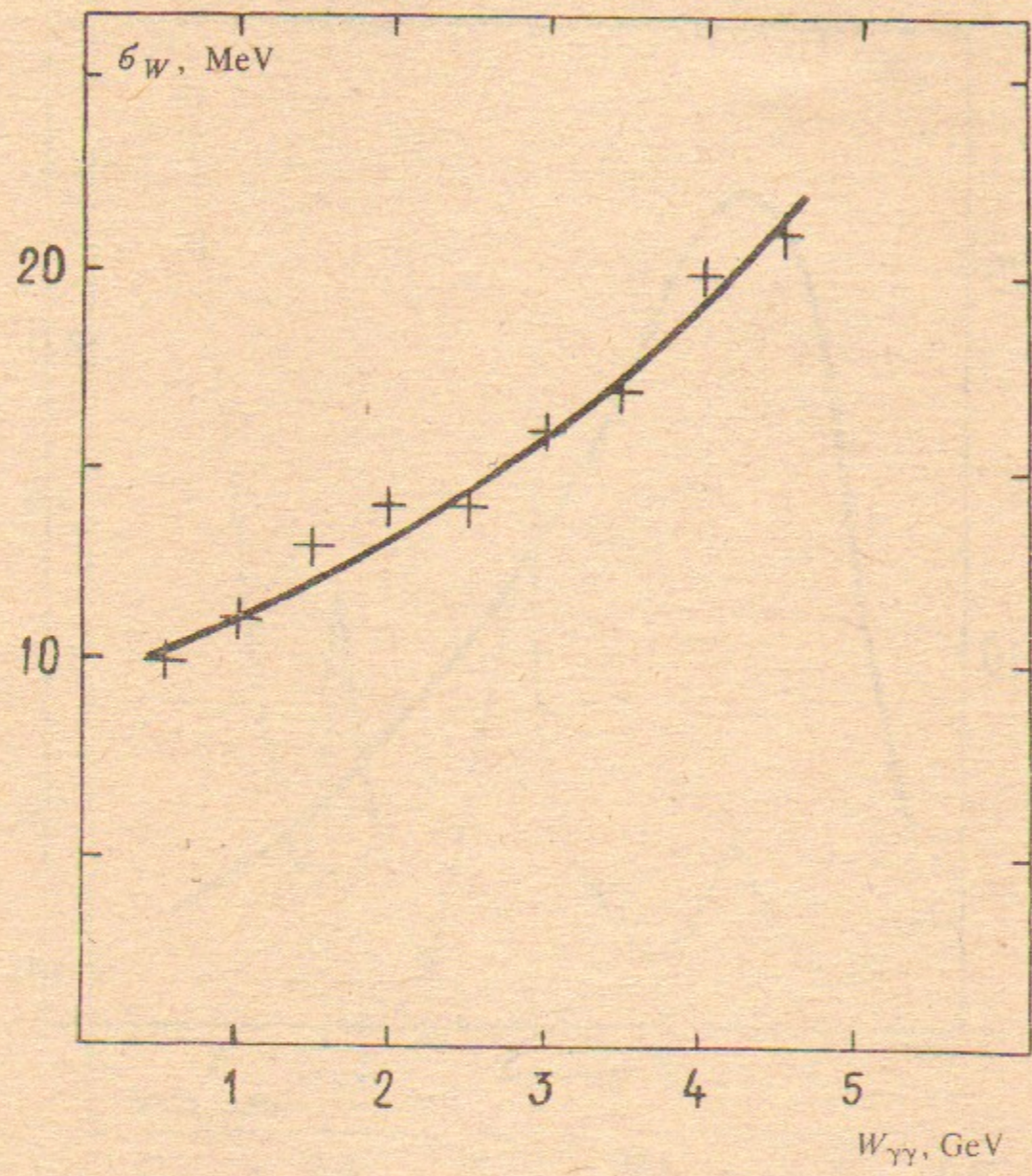


Fig. 4

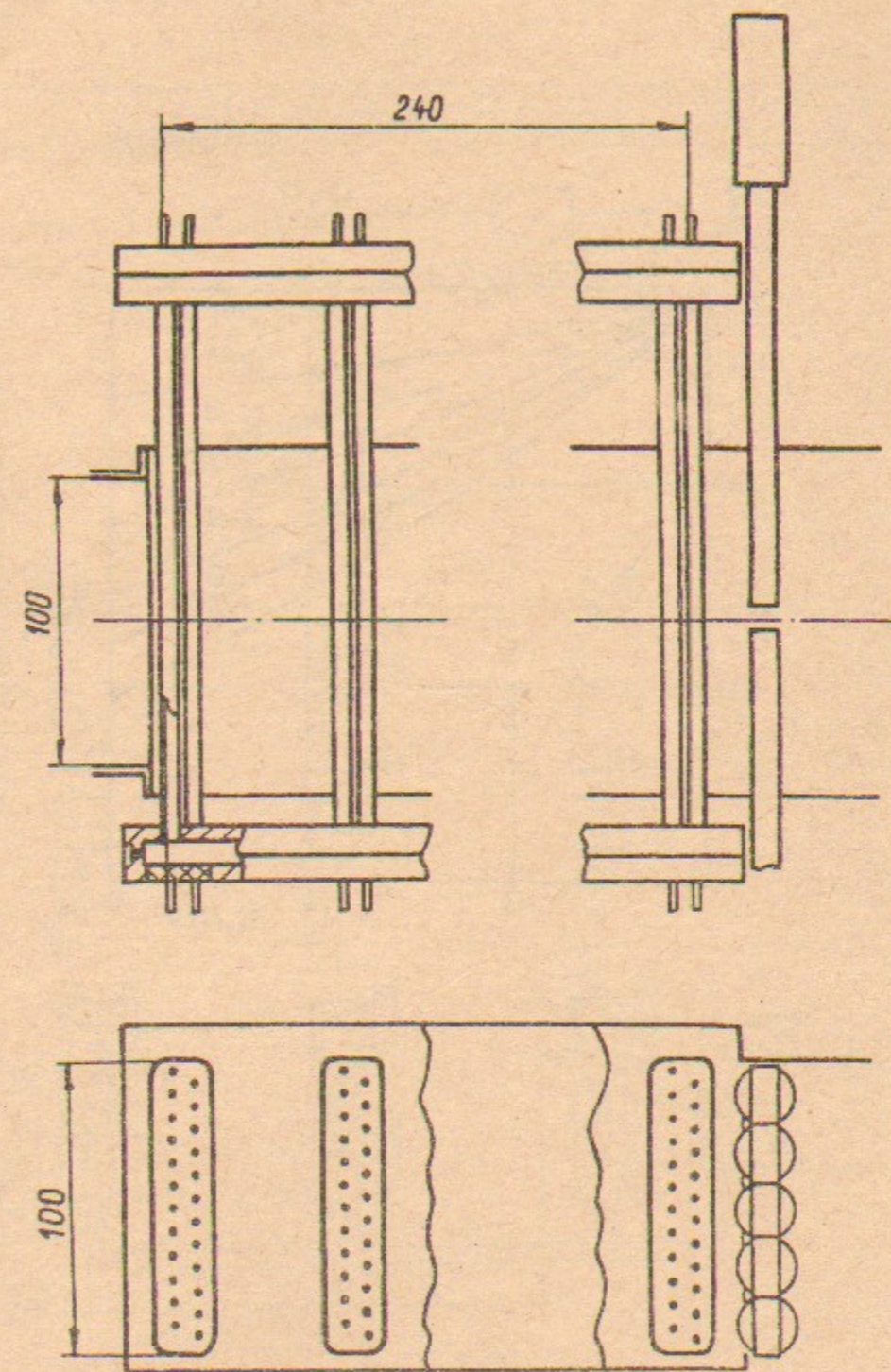


Fig. 5

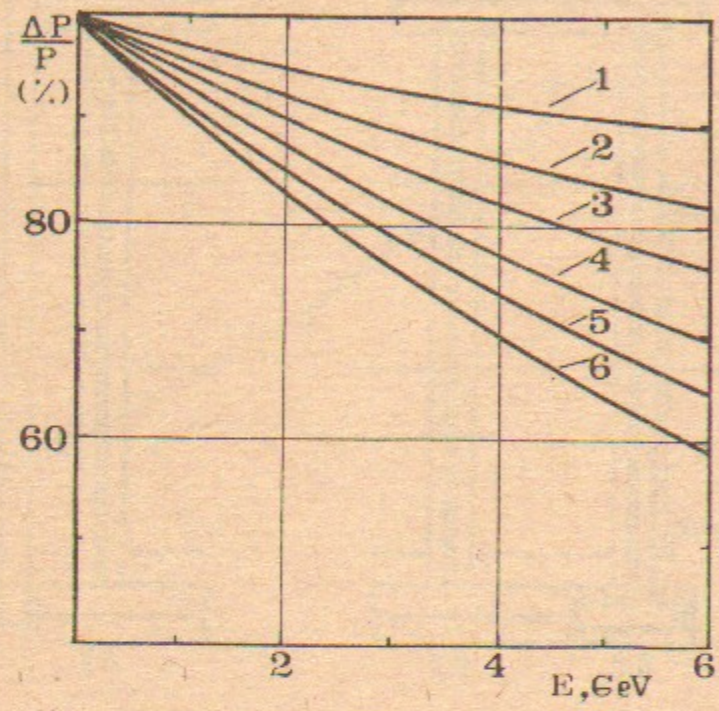


Fig. 6

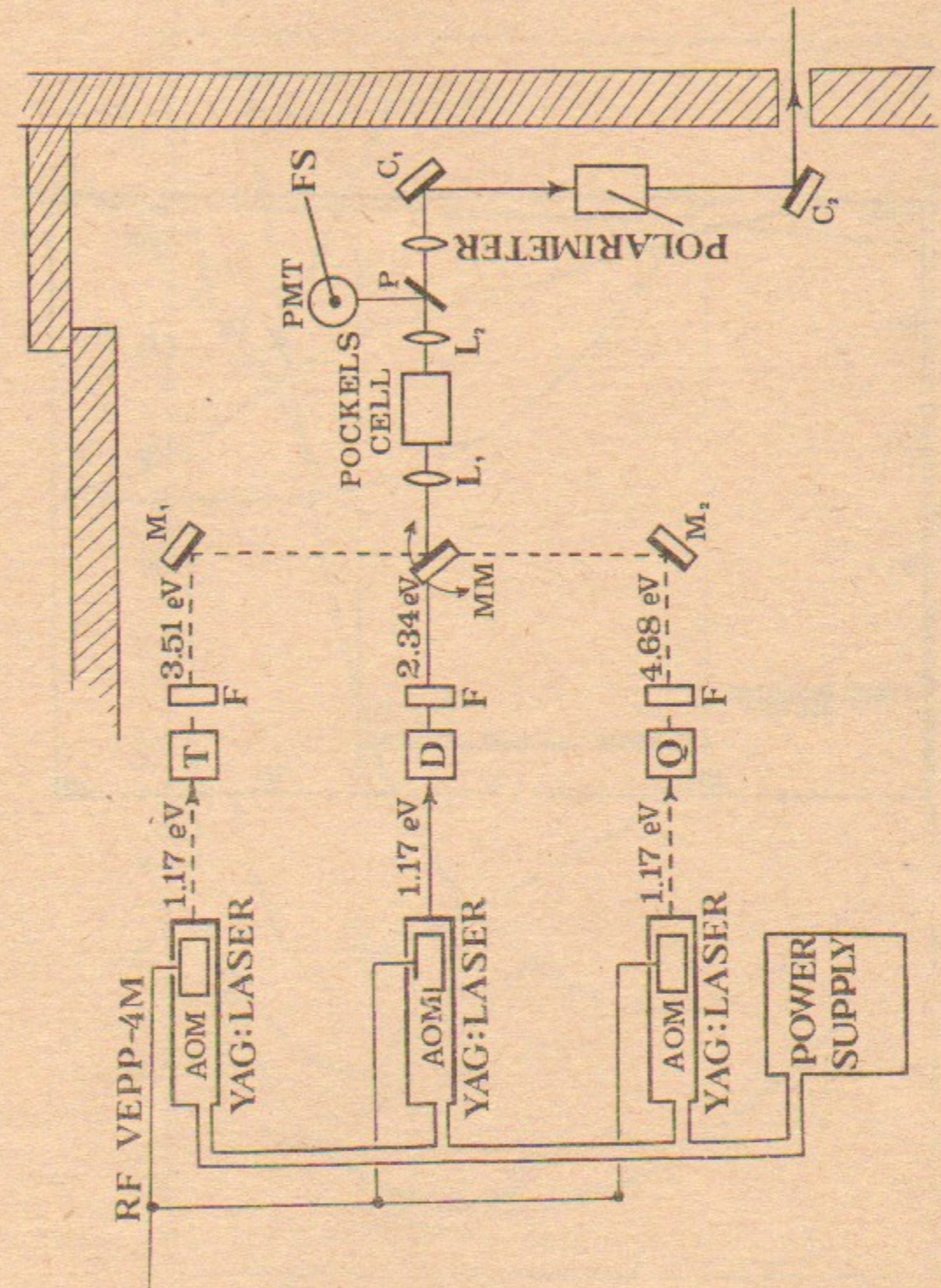


Fig. 7

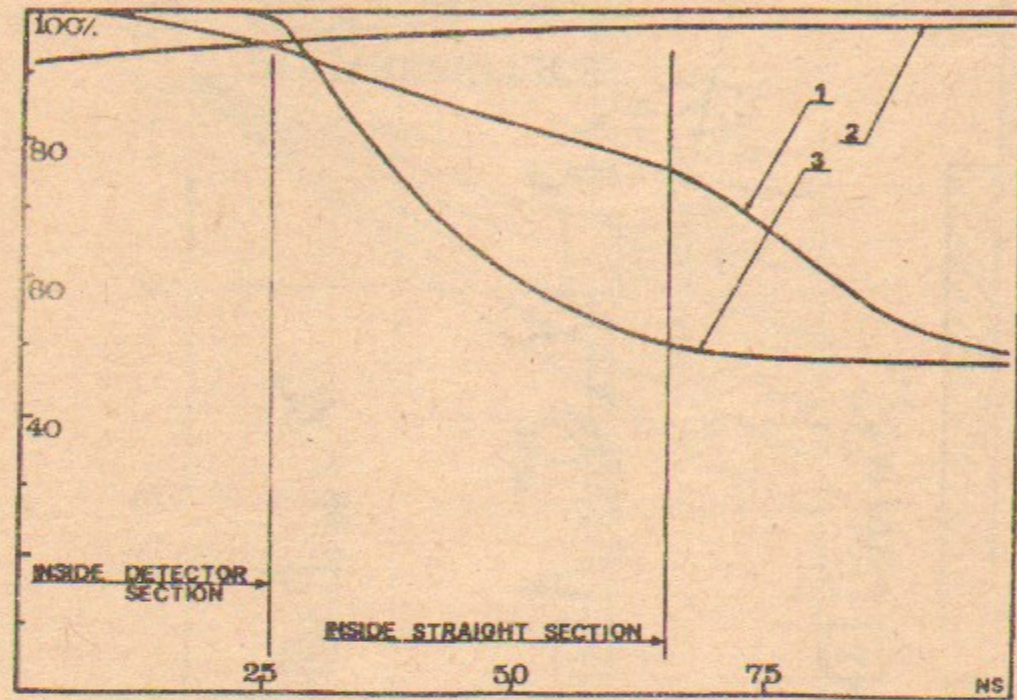


Fig. 8

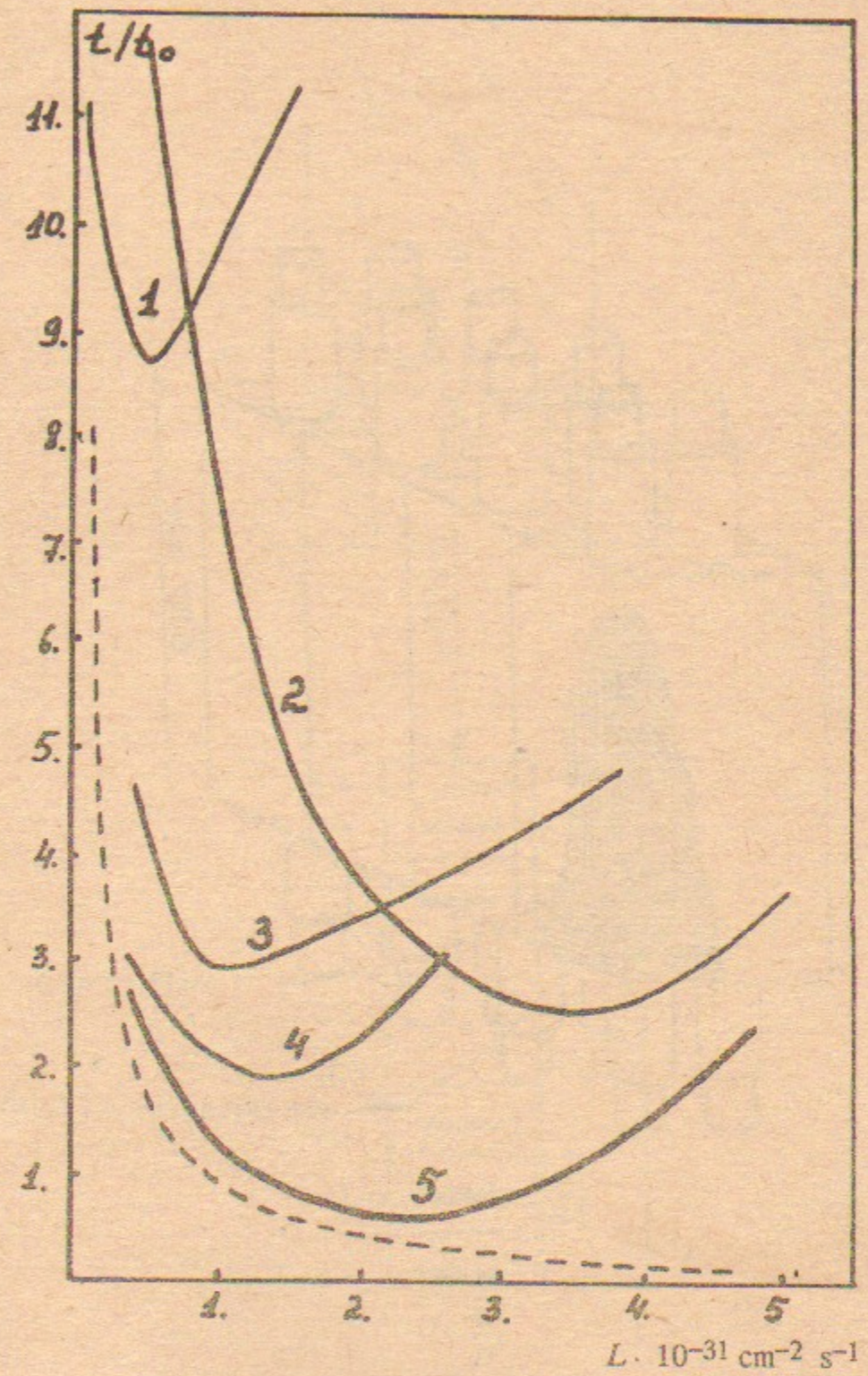


Fig. 9

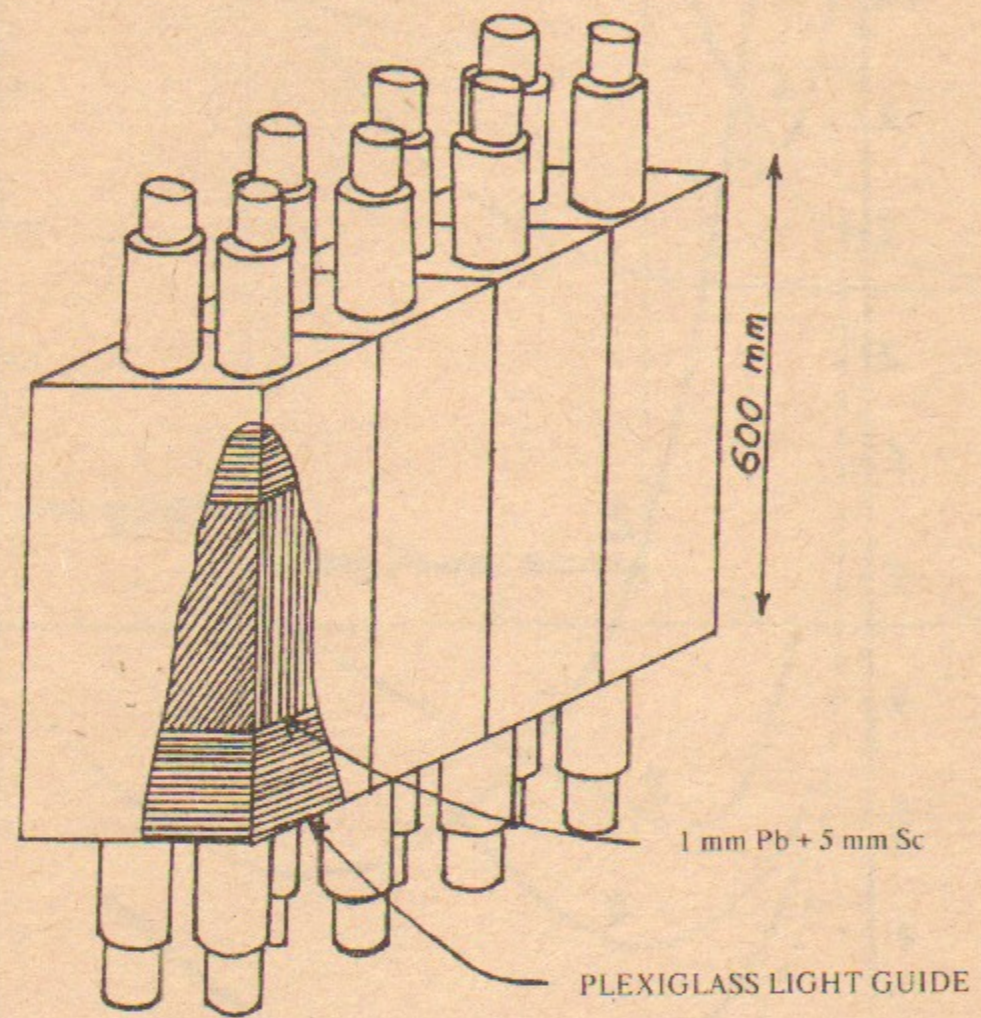


Fig. 10

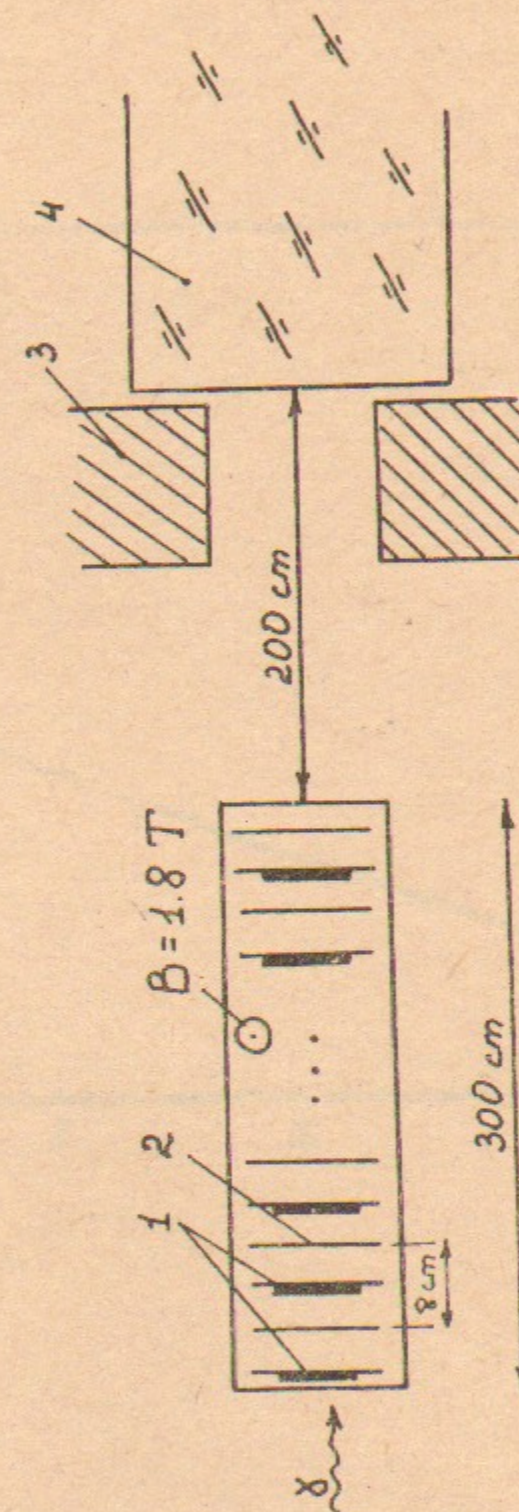


Fig. 11

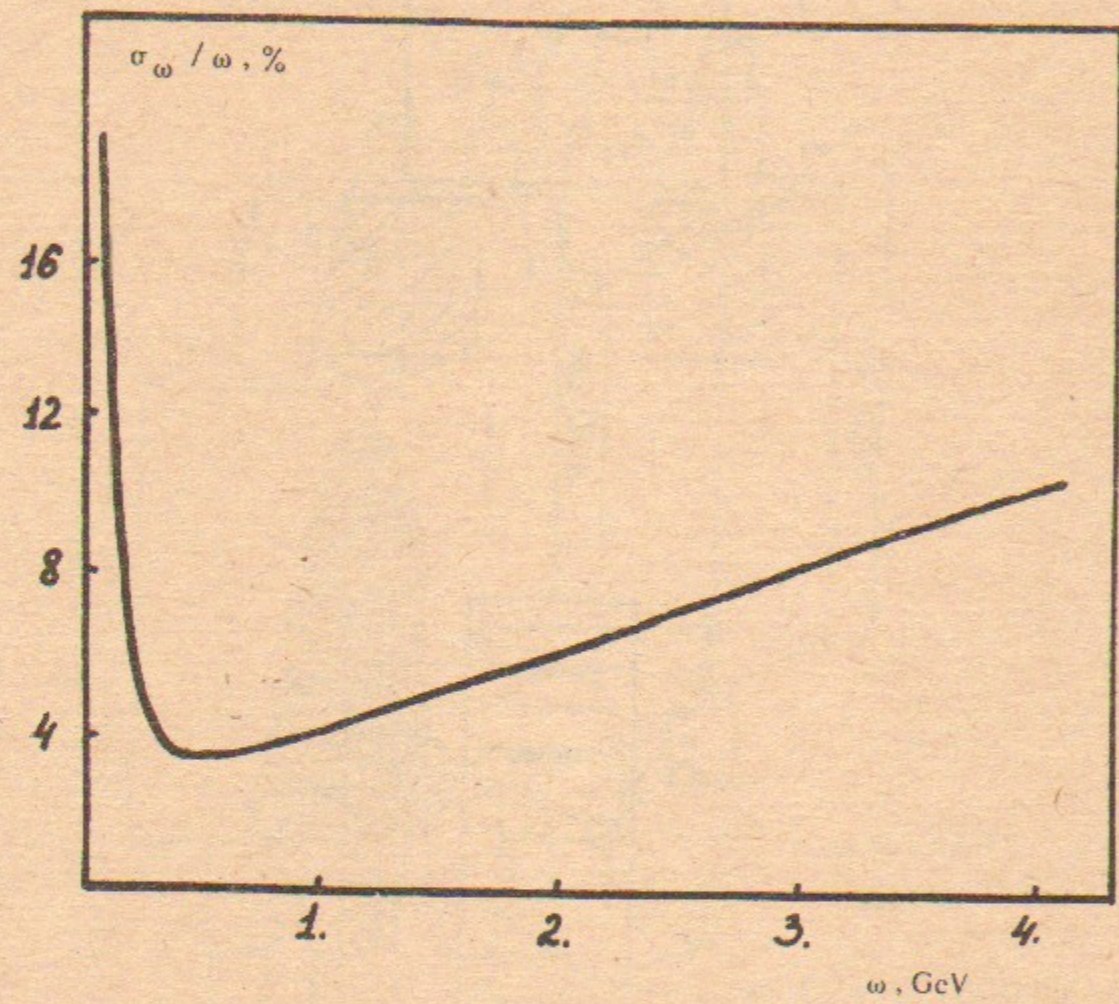


Fig 12

V.M.Aulchenko, B.O.Baibusinov, S.E.Baru, A.E.Bondar,  
A.G.Chilingarov, G.S.Filimonov, G.Ya.Kezerashvili,  
G.M.Kolachev, A.M.Milov, T.A.Purlatz, L.V.Romanov,  
N.I.Root, G.A.Savinov, V.V.Serbo, B.A.Shwartz, V.M.Titov,  
A.E.Undrus, A.P.Usov, V.N.Zhilich, A.A.Zholentz  
H.Calen, S.Kullander

DETECTOR "KEDR" TAGGING SYSTEM  
FOR TWO-PHOTON PHYSICS

В.М.Аульченко, Б.О.Байбусинов, С.Е.Бару, А.Е.Бондарь,  
А.Г.Чилингаров, Г.С.Филимонов, Х.Кален, Г.Я.Кезерашвили,  
Г.М.Колачев, С.Куландер, А.М.Милов, Т.А.Пурлац, Л.В.Романов,  
Н.И.Родт, Г.А.Савинов, В.В.Сербо, Б.А.Шварц, В.М.Титов,  
А.Е.Ундрус, А.П.Усов, В.Н.Жилич, А.А.Жоленц

СИСТЕМА РЕГИСТРАЦИИ РАССЕЯННЫХ ЭЛЕКТРОНОВ ДЕТЕКТОРА  
"КЕДР" ДЛЯ ИЗУЧЕНИЯ ДВУХФОТОННЫХ ПРОЦЕССОВ

Препринт 91-49

Работа поступила 6 мая 1991 г.

Ответственный за выпуск С.Г.Попов  
Подписано к печати 6 мая 1991 г.  
Формат бумаги 60x90 1/16. Объем 2,7 печ.л., 2,2 уч.-изд.л.  
Тираж 290 экз. Бесплатно. Заказ № 73

Ротапринт ИЯФ СО АН СССР, г.Новосибирск, 90.